ANNUAL REVIEWS

Annual Review of Fluid Mechanics

The Flow Physics of Face Masks

Rajat Mittal,[1,2] Kenneth Breuer,[3] and Jung Hee Seo[1]

[1]Department of Mechanical Engineering, Johns Hopkins University, Baltimore, Maryland, USA; email: mittal@jhu.edu

[2]School of Medicine, Johns Hopkins University, Baltimore, Maryland, USA

[3]Center for Fluid Mechanics, School of Engineering, Brown University, Providence, Rhode Island, USA

ANNUAL REVIEWS **CONNECT**

www.annualreviews.org

- Download figures
- Navigate cited references
- Keyword search
- Explore related articles
- Share via email or social media

OPEN ACCESS

Keywords

COVID-19, respiratory infection, SARS-CoV-2, coronavirus, airborne transmission

Abstract

Although face masks have been used for over a century to provide protection against airborne pathogens and pollutants, close scrutiny of their effectiveness has peaked in the past two years in response to the COVID-19 pandemic. The simplicity of face masks belies the complexity of the physical phenomena that determine their effectiveness as a defense against airborne infections. This complexity is rooted in the fact that the effectiveness of face masks depends on the combined effects of respiratory aerodynamics, filtration flow physics, droplet dynamics and their interactions with porous materials, structural dynamics, physiology, and even human behavior. At its core, however, the face mask is a flow-handling device, and in the current review, we take a flow physics–centric view of face masks and the key phenomena that underlie their function. We summarize the state of the art in experimental measurements, as well as the growing body of computational studies that have contributed to our understanding of the factors that determine the effectiveness of face masks. The review also lays out some of the important open questions and technical challenges associated with the effectiveness of face masks.

1. INTRODUCTION

Respiratory droplets ranging in size from $\mathcal{O}(0.1\,\mu m)$ to $\mathcal{O}(1,000\,\mu m)$ are expelled from the mouth and nose of people during various expiratory activities (Duguid 1946, Loudon & Roberts 1967, Papineni & Rosenthal 1997, Chao et al. 2009, Gralton et al. 2011, Johnson et al. 2011) with velocities that may exceed 10 m/s (Zhu et al. 2006, Gupta et al. 2009, Abkarian et al. 2020). For individuals suffering from respiratory infections such as COVID-19, these droplets become carriers of the infection-causing pathogen and serve as vectors for disease transmission. Droplets expelled from the mouth and nose are subject to evaporation (Wells 1934) at rates that depend primarily on relative humidity and temperature (Xie et al. 2007), and this results in a reduction in droplet size and even the formation of droplet nuclei. Given the high density of the droplets in comparison with the surrounding air, droplets with diameters larger than about 10 μm sediment quickly, while smaller droplets and droplet nuclei become aerosolized (i.e., suspended in the air for many minutes or hours) (Fennelly 2020, Wang et al. 2021). These small particles may be carried far by air currents (Mittal et al. 2020a, Bourouiba 2021) and inhaled deep into the lungs of others (Dua et al. 2020, Darquenne 2012). These characteristics of aerosolized respiratory particles are central to the danger posed by airborne transmission, that is, transmission through pathogen-bearing respiratory aerosol particles emitted by infected persons and inhaled by others (Tang et al. 2021). Indeed, after some controversy (Lewis et al. 2020, Mandavilli 2020, Randall et al. 2021), there has emerged a consensus that airborne transmission constitutes the dominant pathway for the spread of COVID-19 (Morawska & Milton 2020, Greenhalgh et al. 2021, Wang et al. 2021), as it does for many other diseases such as tuberculosis, measles, and chickenpox (Ather et al. 2020).

Face masks offer one of the best defenses against this modality of transmission by trapping and reducing the number of aerosolized particles inhaled by a susceptible person (inward protection), as well as the number of droplets emitted by an infected host into his/her surroundings (outward protection). The recurring surges in infections driven by new SARS-CoV-2 (severe acute respiratory syndrome coronavirus 2) variants even as late as two years into the pandemic (Corum & Zimmer 2022), as well as the recent history of other epidemics (Guarner 2020) driven by respiratory infections, suggest that the months and years ahead will likely see face masks retain their status as the most used medical device in the world. Understanding the physics that underpins the effectiveness of face masks as a defense against airborne pathogens is, therefore, more important than ever.

A face mask is essentially an air-handling device, and flow physics therefore plays a central role in every facet of its design and function. However, for such a seemingly simple device, the fluid dynamics of face masks is strongly coupled with phenomena in several other physical domains such as nano-/microfluid dynamics, structural dynamics, droplet and particle dynamics, and even electrostatics. The scales in the problem also range from nanometers (the size of the virus and the fiber diameter in some face masks) to meters (the distance traveled by a respiratory jet). It is therefore not surprising that despite attempts by researchers from a variety of disciplines, significant knowledge gaps persist regarding the fundamental fluid dynamics of face masks.

The use of the face mask as a protective medical device dates back centuries, originating before any modern understanding of infection or airborne transmission of disease. The long-beaked masks from fourteenth-century Europe stuffed with herbs and spices were thought to protect the user from the Black Plague (Mussap 2019). Of course, the more recent literature, based on modern scientific study, has addressed many aspects of the flow physics and filtration performance of face masks; however, the COVID-19 pandemic has resulted in a veritable explosion of new studies that have employed state-of-the-art methods. Given the nature of the topic, these papers have appeared not only in journals devoted to fluid mechanics and aerosol science but also in general science publications and in health science–related publications. What is lacking, however, is

a review that summarizes this large and diverse body of literature from a fluid dynamics–centric perspective. The current review focuses on what is known, measured, and simulated in the arena of face mask fluid dynamics, as well as the limits of our knowledge and potential opportunities for scientific study and discovery in this arena.

2. FLOW PHYSICS OF FACE MASK FILTRATION

Various public health organizations and regulatory agencies around the world have set definitions and standards for the performance of face masks (Lepelletier et al. 2020, Das et al. 2021, Ju et al. 2021). While these might differ in specific details, overall there are three main categories: fitted facepiece (FFP) masks (which includes N95 masks), medical or surgical masks, and cloth masks. FFP masks are further categorized based on their filtering performance; FFP1, FFP2, and FFP3 masks filter more than 80%, 94%, and 99% of aerosols, respectively. Irrespective of face mask type, all face masks function as fibrous aerosol filters (see **Figure 1*a*,*b***), and studies of aerosol filtration by fibrous filters go at least as far back as the work of Langmuir in the early 1940s (Langmuir 1942). The key performance metrics for any aerosol filter are the particle filtration efficiency (FE), which is defined as $FE = 1 - C_d/C_u$ (where C_d and C_u are aerosol concentrations downstream and upstream of the filter, respectively), and the pressure drop across the filter $\Delta P_f = (P_u - P_d)$. Both of these are related to the material and topological properties of the filter. The topological properties of a fibrous medium are typically defined by the following parameters: filter thickness, fiber diameter d_f, and packing density, which is the ratio of the volume of the fibers to the volume of the fibrous
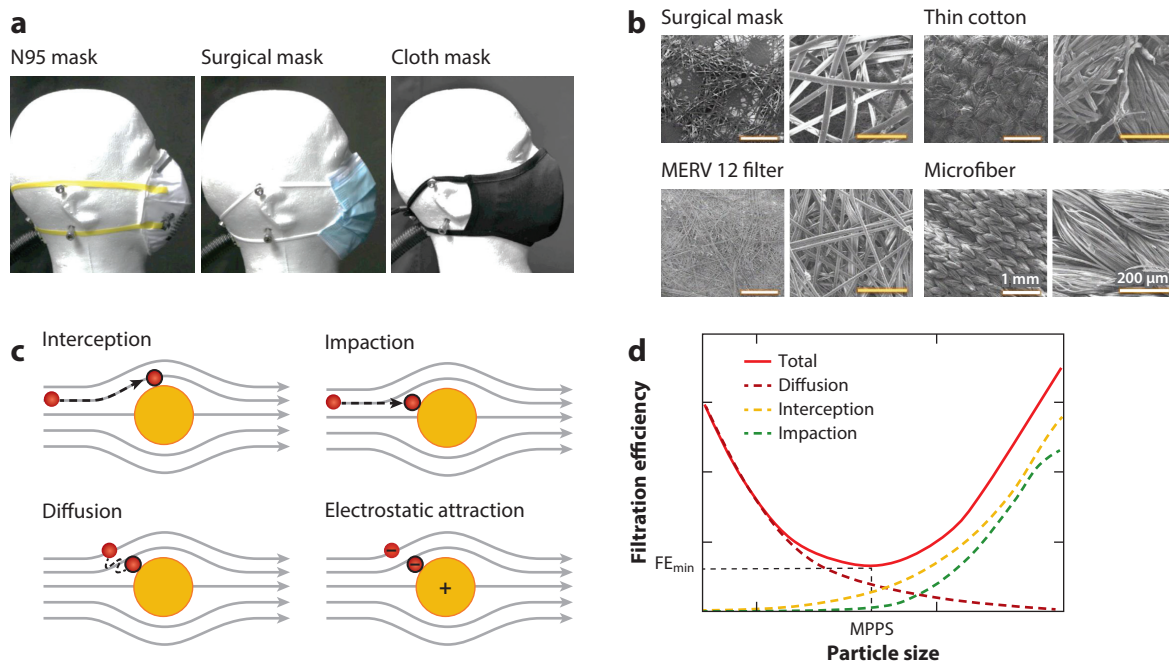
Figure 1

(*a*) Three face masks used widely during the COVID-19 pandemic: N95, surgical mask, and cloth mask. Panel adapted from Koh et al. (2022) with permission from Elsevier. (*b*) Fibrous microstructure of filter materials. Panel adapted from Pan et al. (2021) with permission of Taylor & Francis. (*c*) The various particle-trapping mechanisms associated with fibrous filters. (*d*) Combined action of particle-trapping mechanisms on the FE. Abbreviations: FE, filtration efficiency; MPPS, most penetrating particle size.

media. In addition, the topology of the fibers (for instance, woven versus nonwoven) also plays an important role in the filtration performance of the filter (Ju et al. 2021). Face masks can be made of a single layer (such as many cloth masks) or they can be multilayered. For instance, most commercial surgical masks have three layers where the middle layer is the filter medium, the inner layer is for absorbing moisture, and the outer layer repels water. Similarly, N95 masks have an outer filter and inner layers with different fiber properties and configurations (Das et al. 2021, Ju et al. 2021).

The physical principles that underpin the trapping of particles by a fibrous medium have been well established and these involve particle diffusion, inertial impaction, interception, and electrostatic attraction (see **Figure 1c**) (Hinds 1999). Diffusion involves particles with diameters less than about 0.1 μm that come in contact with a fiber due to Brownian motion. Diffusion-based particle capture is determined by the fiber Péclet number $Pe = d_f U/D$ (where U is the flow velocity and D is the diffusion coefficient) and the hydrodynamic factor (Lee & Liu 1982), which accounts for the modification of flow due to adjacent fibers and is usually expressed in terms of the volumetric packing density. Particles with significant inertia do not follow the flow streamlines that go around the fibers and may consequently impact and stick to the fiber. This occurs mostly for particles with diameters d_p greater than about 1 μm, and the importance of inertial impaction is primarily determined by the particle Stokes number, which for particle–fiber interaction is expressed as $S = \rho_p d_p^2 U/(18\mu d_f)$, where ρ_p and d_p are the particle density and diameter, respectively, and μ is the fluid viscosity. Interception occurs for particles that follow streamlines but approach close enough to the fiber to be captured. This mechanism is governed by the interception parameter $R = d_p/d_f$ and typically occurs for particle sizes greater than about 0.1 μm. Electrostatic collection occurs if the fiber or the particle, or both, carry charge and is particularly important for very small (nanoscale) particles. For instance, the filter layer of N95 masks is made of polarized (electret) fibers (Van Turnhout et al. 1981), which are known to increase the masks' FE (Ju et al. 2021).

The overall FE of a mask material is a combination of these different mechanisms. As shown in **Figure 1d**, the complementary effects of diffusion-induced trapping on the one hand (it diminishes as particle size increases beyond 0.1 μm) and impaction and interception on the other (they become increasingly important for particle sizes greater than about 0.1 μm) result in the characteristic U-shaped curve of FE with particle size (Lee & Liu 1982, Hinds 1999, Zangmeister et al. 2020), with a minimum that is identified as the most penetrating particle size (MPPS) and a corresponding minimum FE denoted by FE_{min}. MPPS for most materials that constitute face masks including N95, surgical masks, and common fabric masks ranges from 0.1 to 0.5 μm, but minimum FE ranges from about 95% for the N95 (hence the name) to about 30% and 20% for surgical and common fabric-based mask materials, respectively (Zangmeister et al. 2020, Drewnick et al. 2021). We note here that while MPPS and FE_{min} may be convenient parameters to characterize the performance of a face mask material, respiratory ejecta/aerosols contain particles/droplets that range in size from less than 1 μm to $\mathcal{O}(100)$ μm. Thus, it is the net filtration over this entire particle size range that is relevant for infection transmission, and this overall efficiency is, by definition, larger than FE_{min} (Mittal et al. 2020a).

In addition to the properties of the filter material and particle size, FE also depends on the through-flow velocity (note that flow velocity appears in both the Péclet number and the Stokes numbers above). FE typically decreases with increasing flow velocity (Kwong et al. 2021), and face mask efficiency during talking, coughing, and exercise would therefore be expected to be lower than it is during normal breathing. Temperature, humidity, flow unsteadiness, and the charge status of the filter also modify the FE of face masks, but these factors are generally small compared to the effect of peripheral leaks from the masks (see Sections 4 and 5.1 and Kwong et al. 2021).

The pressure drop across a face mask determines the effort exerted by a person to breathe through the mask and is considered a key measure of the breathability of the mask. The pressure
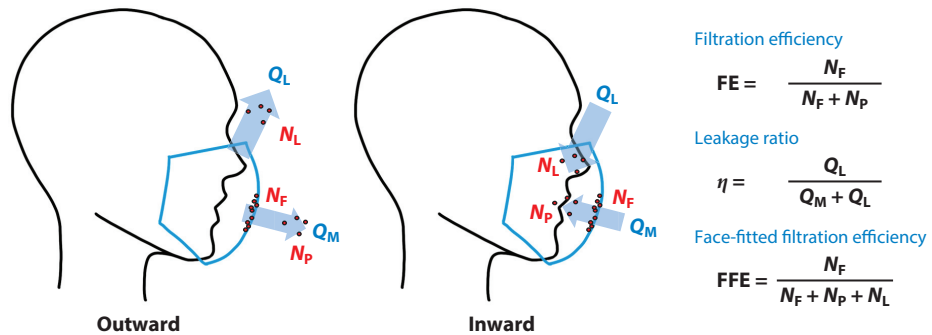
drop across a face mask can be determined via Darcy's law $\Delta P_f = T_f \mu U/k$, where k is the permeability of the mask material and T_f is the filter thickness (Hinds 1999). At high flow rates, nonlinear effects may be important and can be introduced via the so-called Darcy–Forchheimer model (Bejan 2013). Various regulatory bodies have established breathability standards for face masks (Kwong et al. 2021); for instance, in the United States, the National Institute for Occupational Safety and Health requires N95 face masks, with no face seal leaks, to have a maximum pressure drop of 343 Pa (245 Pa) for inhalation (exhalation) at an average through-flow velocity of 9.4 cm/s (Kwong et al. 2021), which corresponds to a ventilation rate in a state of vigorous physical exertion. It should be noted that at high flow velocities such as those associated with coughing and sneezing, the linear Darcy's law might not hold and nonlinear inertial effects should be included. Not surprisingly, FE and pressure drop are correlated with one another since both increase with increasing packing density. Thus, increasing FE without a concomitant increase in the pressure drop is one of the key challenges in the development of effective materials for face masks (Mao & Hosoi 2021).

The estimation of FE and ΔP_f has been the subject of numerous studies, and recent articles by Kwong et al. (2021) and Mao & Hosoi (2021) summarized measurements for a wide variety of face masks ranging from N95 and surgical masks to cloth masks. While we do not discuss in detail the methods and results described in these studies, it is worth pointing out the tremendous variability in the results reported for non-FFP face masks, which indicates the complexity inherent in the underlying physical phenomena and in conducting these measurements. Taking only surgical masks as an example—since they are manufactured commercially and expected to adhere to certain standards—Kwong et al. (2021) found (figure 5 in their paper) that FE varies from 17% to 95%. This large variability is primarily due to differences in (*a*) the face mask materials and their condition; (*b*) the methods used to generate and collect particles in the experimental tests, and the inherent uncertainty in these measurements; (*c*) the face flow velocities at which the measurements are made; (*d*) the particle size ranges employed; and (*e*) how FE is defined. Thus, despite over half a century of research and analysis, measurements of FE for mask materials remain a challenge. However, notwithstanding this large variability, several useful trends do appear: N95 masks have a FE_{min} that is indeed close to 95%; minimum FEs of surgical masks average out in the 50% range; nonwoven fabrics provide, in general, a higher FE than woven fabrics; and some nonwoven cloth fabrics perform as well as surgical masks (Ju et al. 2021).

All of the above measurements, however, correspond to the situation when there are no face seal (peripheral) leaks from the mask. Such leaks can significantly reduce the filtration performance of masks, and this issue is addressed in the next section, as well as later in the article.

3. FITTED FILTRATION EFFICIENCY

Fitted FE (FFE) corresponds to the filtration efficiency of a face mask when it is worn by (or fitted on) a person (Tuomi 1985, van der Sande et al. 2008). The key difference between FE and FFE is due to the aerosol particles that leak through the gaps that appear between the periphery of the mask and the face when the mask is worn by a person (Hill et al. 2020, Bagheri et al. 2021b). As is discussed below, estimation of this particle leakage is highly nontrivial. The difference between FE and FFE is the number of aerosol particles/droplets (N_L) that leak through the gap (**Figure 2**). If all the particles follow streamlines, then N_L would be directly proportional to the leakage flow rate Q_L, and this leads to the following: FFE = FE$(1 - \eta)$, where η is the ratio of flow leakage volume flux to total flux. However, since only the small particles follow streamlines, and respiratory aerosols, especially during exhalation, can potentially contain larger droplets, the above estimate may be considered as a lower bound on FFE. In contrast, the larger particles contained in respiratory droplets/aerosols are driven by inertia, and in the extreme case, all of

$$\text{Filtration efficiency}$$
$$FE = \frac{N_F}{N_F + N_P}$$

$$\text{Leakage ratio}$$
$$\eta = \frac{Q_L}{Q_M + Q_L}$$

$$\text{Face-fitted filtration efficiency}$$
$$FFE = \frac{N_F}{N_F + N_P + N_L}$$

Outward   **Inward**

Figure 2

Flow and droplet transport through face masks, and the definition of various mask efficiency metrics. FE, η, and FFE are the filtration efficiency of the mask, the leakage flow ratio, and the fitted filtration efficiency, respectively. The parameters appearing in the above expression are N_P, N_F, and N_L, which are the number of droplets that pass through the mask, are captured by the mask, and leak through the gaps, respectively. Q_M is the flow rate through the mask, and Q_L is the leakage flow rate through the peripheral gap.

these particles could impact the face mask (especially during expiration, where the expiratory jet is pointed directly toward the mask fabric) and undergo filtration. For these particles, FFE is equal to FE, and this therefore represents the upper bound for FFE. Given the broad range of particle sizes that are possible in respiratory aerosols/ejecta (Gralton et al. 2011), the actual FFE will lie somewhere within these two bounds.

The dependency of FFE on particle adherence to streamlines can be modeled through the introduction of a parameter (here, σ) representing the fraction of particles/droplets that follow or adhere to streamlines. The parameter σ is expected to be a function of the particle Stokes number, which itself depends on particle size and velocity. Assuming, for instance, a typical flow velocity of 5 m/s, the particle Stokes number ranges from $\mathcal{O}(1)$ to $\mathcal{O}(100)$ for particle size ranges from 0.1 to 10 μm, respectively. Particles with Stokes numbers less than 1 would follow the streamlines closely and σ for these particles will be close to 1. With this parameter, FFE can be expressed as

$$FFE = \sigma FE(1 - \eta) + (1 - \sigma)FE = FE(1 - \eta\sigma). \qquad 1.$$

Concealed within the apparent simplicity of the above expression is a high level of complexity since all three parameters, FE, η, and σ, that appear in the expression for FFE have complex dependencies on several factors/variables (see **Table 1**). Amplifying this complexity is the fact that most of the factors and variables indicated in the table themselves vary over large ranges.

Table 1   Dependencies of the variables involved in FFE on various underlying factors/variables[a]

	FE	η	σ
Mask type and condition	✓	✓	—
Aerosol particle size	✓	—	✓
Face velocity or ventilation rate	✓	✓	✓
Face topology	—	✓	—
Type of expiratory activity	—	✓	—
Inhalation or exhalation	—	✓	✓

Abbreviations: η, leakage ratio; σ, streamline adherence ratio; FE, filtration efficiency; FFE, fitted FE.
[a]See Equation 1.

For instance, the ventilation rate for breathing varies over a factor of 15 or more depending on the level of physical exertion (Mittal et al. 2020a). The aerosol particle size distribution is key to the determination of FE and σ, and this distribution depends on the type of expiratory activity (breathing, talking, coughing and sneezing), and even varies significantly from one individual to another (Asadi et al. 2019). Significant effort has been invested in measuring the aerosol particle size distribution for these different expiratory activities since the 1940s (Mittal et al. 2020b). However, despite this concerted effort, there remains significant uncertainty regarding this most fundamental of measures associated with respiratory aerosols (Gralton et al. 2011, Bagheri et al. 2021a, Pöhlker et al. 2021).

Of particular interest in the context of respiratory infections such as COVID-19 is the difference between inward protection (during inhalation) and outward protection (during exhalation) offered by face masks; the former is the protection afforded by the mask to the wearer, while the latter is the protection afforded from the wearer to people in close proximity. Outward protection has garnered particular attention during the COVID-19 pandemic due to the significant role that aerosol transmission from asymptomatic (and presymptomatic) infected hosts has played in driving this pandemic (Mittal et al. 2020b, Verma et al. 2020, Greenhalgh et al. 2021).

The expression for FFE in Equation 1 offers a useful way to examine the fundamental difference between inward and outward protection. Due to evaporation and settling, the size of inhaled respiratory aerosol particles is expected to be smaller than that of exhaled particles (Bagheri et al. 2021b). This, combined with the fact that mask through-flow velocities during inhalation tend to be on the lower end of the range, would lead to a σ for inhalation that is close to unity, thereby resulting in an FFE that is closer to its lower bound. In contrast, during exhalation, respiratory particle/droplet size can range from less than 1 μm to $\mathcal{O}(100)$ μm (the large particles result from expiratory activities such as talking, coughing, and sneezing). This, coupled with the relatively high velocities of the expiratory jet directed toward the mask, would result in a σ for exhalation that is less than (possibly significantly) unity. However, the buildup of pressure inside the mask during exhalation is expected to enhance leakage (i.e., increase η), and this trend could counteract the expected decrease in σ, resulting in an FFE for exhalation that is lower than that for inhalation. In the following sections, we provide more details about the state of our knowledge regarding inward and outward protection associated with face masks.

4. INWARD PROTECTION

Inward protection from infection depends on the effectiveness of the mask in trapping droplets containing infectious agents and, thus, preventing them from entering the respiratory tract during inhalation, through either the mouth or nose. From a fluid mechanics perspective, inhalation can be modeled as a short-duration sink flow, drawing fluid in uniformly from the region adjacent to the face. Typical flow rates for adults range from about 5 L/min to 100 L/min, depending on the activity level (Mittal et al. 2020a).

Inward protection provided by a mask can be defined by FFE or by a protection factor—the ratio of the total ambient aerosol concentration to the concentration inside the mask (Lee et al. 2008), which is equal to $(1-\text{FFE})^{-1}$. As indicated in **Table 1**, this metric depends on, among other things, the inhalation flow rate and the size distribution of particles in the vicinity of the wearer (Bałazy et al. 2006). Some situations, such as close-up conversations, smoky rooms, and construction sites, are characterized by high particulate loading with a significant fraction of large (liquid or solid phase) particles (e.g., Steinle et al. 2018). In contrast, in situations with moderate social distancing between people, heavy droplets have more time to sediment, and the flow will be dominated by smaller aerosol particles. The streamline adherence fraction σ for these situations will therefore be close to unity. Quantitative measurements of inward protection and the
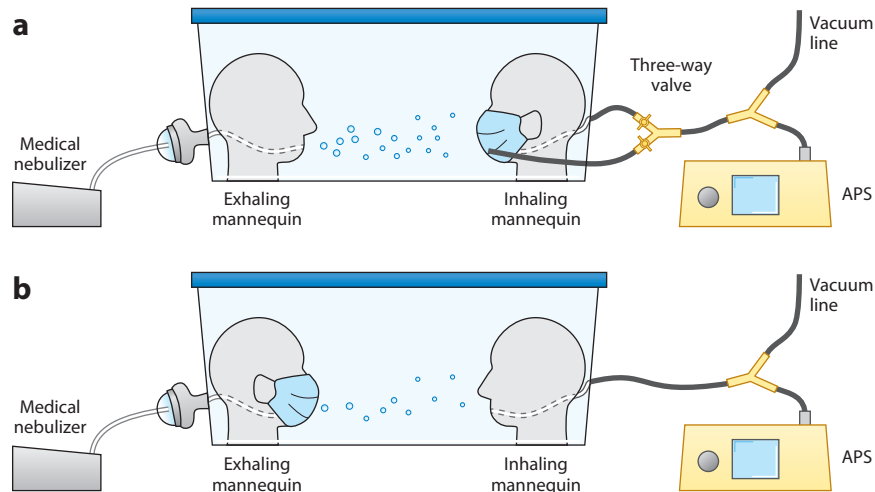
Figure 3

A typical sealed testing apparatus used to measure mask performance and leakage. (*a*) For measuring inward protection, air samples are taken from both in front of and behind the mask, and subsequently analyzed by the aerodynamic particle sizer (APS) spectrometer. (*b*) For measuring outward protection, a single sampling location in the airway of the inhaling mannequin is used to sample the aerosol content emitted by the exhaling mannequin. Figure adapted from Pan et al. (2021) with permission of Taylor & Francis.

effectiveness of masks have been conducted for many years, initially motivated by the protection of health care workers from infection during dental procedures (e.g., Pippin et al. 1987), then in the early 2000s in response to the threat of airborne infection during the SARS (severe acute respiratory syndrome) epidemic of 2003 (e.g., Lee et al. 2008), and most recently due to the COVID-19 pandemic.

Several studies of inward protection have employed mannequins inside a closed chamber filled with aerosol-laden gas (e.g., Pippin et al. 1987, Bałazy et al. 2006, Lee et al. 2008) (**Figure 3a**). The inward breathing (usually simplified using a steady flow) draws air in through the mask, and the inhaled gas is then analyzed for particle density and size distribution. As one might expect, close-fitting masks with thicker mask materials, such as the N95 mask, provide protection factors as high as 90% (Bałazy et al. 2006, Lee et al. 2008).

Surgical masks, which have both thinner mask materials and multiple leakage routes, perform much worse and have much greater test-to-test variability, providing protection factors that range between 8 and 12 times lower than that of N95s (Lee et al. 2008). These reductions in protection factor are also known to be accompanied by increased infection risks (Bagheri et al. 2021b).

With the ever-increasing rise in the abilities of numerical simulations, inward protection has also been studied using computational models. Xi et al. (2020) performed simulations that included the face, mask, and upper airway to quantify droplet deposition with and without a mask. A simple droplet filtration model with a prescribed FE was used in their study, and significant reductions in the airway deposition and lung penetration of the particles were observed with the mask. The study showed that, for inward protection, the filtration effect of the mask is more important than the airflow modification due to the flow resistance introduced by the mask. This suggests that the validation and continued development of more sophisticated filtration models are critical for improved simulation-based studies.

Regardless of the effectiveness of the mask material in reducing droplet transmission, any leakage routes that bypass the mask via a low-pressure drop fluid pathway such as a gap between

the mask and the face will substantially degrade the FFE. Many of the earlier studies on inward protection were conducted using masks with perfect face seals, a condition that is not realistic. Such studies assessed the reduction in mask effectiveness due to leaks by deliberately introducing specified leaks (e.g., Chen & Willeke 1992, Lee et al. 2008, Grinshpun et al. 2009, Lai et al. 2012). While this might not accurately capture the topology of the gaps that occur in practice, some useful insights were obtained from these studies. For instance, Lai et al. (2012) introduced small leakages at the top of the mask beneath each eye and found a reduction in protection factor of approximately 20%. Similarly, Drewnick et al. (2021) found that a 1% leakage area ratio (measured as a fraction of the leakage to mask area) reduced the FE by as much as 50% for small (2.5 μm) aerosols. More realistic leakage tests (Oberg & Brosseau 2008, Grinshpun et al. 2009) have shown that about 5% of aerosols in the ambient environment reached the face via a leakage path around an N95 mask, which is an order of magnitude higher than the percent of aerosols that manage to pass through the mask material. However, this grew to as much as 40% for a surgical mask, presumably due to the larger leakage paths common for loose-fitting surgical masks. Other recent measurements of inward protection that include leakage paths give protection factors that range between 25% and 95% (Pan et al. 2021), and what is clear is that these numbers are very dependent upon the specifics of the material and the leakage paths, which are sensitive to the mask's fit to the face (see **Table 1**). It should also be noted that protection can also decrease as the mask ages due to clogging of the mask material. Reductions of FE of as much as 30% over 10 hours were observed by Lee et al. (2022), although this was for uncertified masks (certified masks exhibited only 4% FE reductions). Numerical simulations by Dbouk & Drikakis (2020) also demonstrated this clogging behavior.

All in all, despite several studies, conclusive statements regarding FFE are difficult to make with authority, and we are limited to more general conclusions such as that masks are more effective in providing inward protection than outward protection, and that respirator-type masks, such as N95, are found to be more effective than surgical masks (van der Sande et al. 2008, Smith et al. 2016) and provided improved protection against infection (Bagheri et al. 2021b).

5. OUTWARD PROTECTION

The outward protection (i.e., protection from the wearer of the mask) is associated with two effects of the face mask: filtration of the virion-bearing aerosol particles from the exhalation respiratory jet, and the modification of the respiratory jet itself. We address both of these effects in the following sections.

5.1. Peripheral Leakage

As with inward protection, the leakage from the peripheral gaps appears as the key factor in outward protection as well; leakage determines not only the FFE of the mask during exhalation but also the topology and characteristics of the outward respiratory jet. The degree of leakage is expected to be larger during exhalation than during inhalation simply because the high pressure generated in the region between the face and the mask during exhalation is expected to push the mask outward, thereby enhancing the leakage. Furthermore, activities such as talking, coughing, and sneezing are primarily expiratory activities, and the higher mask pressures and the dynamic movement associated with these activities are expected to further enhance the leakage.

Quantification of the net leakage flow and of the leakage ratio η is surprisingly challenging for a variety of reasons. First, as shown in **Table 1**, the peripheral leakage depends on several factors, including the type of the mask, how it is worn, the topological characteristics of the wearer's face (Solano et al. 2021), the ventilation rate, and the expiratory activity (breathing, talking, coughing, and sneezing). In experiments, it is difficult to directly measure the size of the small peripheral

gaps between the mask periphery and the wearer's face. Lai et al. (2012) estimated that the degree of protection provided by a mask dropped from close to 100% for a fully sealed mask to about 50% for a normally fitting mask. Most other experiments focused on visualizing the leakage flow (e.g., Tang et al. 2009, Verma et al. 2020) or measuring the particle concentrations of the emitted respiratory particles (Asadi et al. 2019).

Modeling studies have also attempted to incorporate mechanics-based predictions of peripheral gaps into these simulations. One of the earliest computational studies to attempt this modeling was that of Lei et al. (2013), who used a finite-element model to predict the gap between the face and mask, coupled with fluid flow simulations to quantify the leakage flow. Their simulations for the N95 mask indicated that in typical scenarios, 80% of the expiratory flow leaks through the periphery of the mask. The flow through the filter medium and the leakage are determined by the flow resistances of the filter and the leakage gap. Thus, a mask with high FE and low permeability may result in more leakage flow, and simulations show, for instance, that doubling the mask resistance increases the leakage flow ratio from 80% to 90% (Lei et al. 2013).

The key challenges in computational modeling of outward protection are (*a*) predicting the size and conformation of the peripheral gaps correctly, (*b*) simulating the flow through these narrow gaps, and (*c*) modeling flow through the porous material of the face mask. Some studies assume a gap of a prescribed size, but this sidesteps the issue of predicting the gap. An interesting study in this context is that of Perić & Perić (2020), who proposed a simple 1D model to examine peripheral leakage through peripheral gaps of a prescribed size. The flow and pressure loss across the peripheral gaps were modeled as a Poiseuille flow. The Darcy–Forchheimer (Hinds 1999) model was used for the pressure drop across the mask, and values of the viscous porous resistance typical for face masks were employed. The simulations showed that even a 1-mm gap that is 5 cm long could result in 50% leakage. Results of these 1D models were found to compare well with 3D Navier–Stokes simulations, thereby indicating the utility of such methods for design and analysis.

Solano et al. (2021) introduced a computational framework to predict the effect of face shape and topology on the formation of peripheral gaps. The framework employs a quasi-static mechanical model of the face mask fitted to face topologies that are generated using the Basel Face Model (BFM) (Paysan et al. 2009), a public database of face scans. Solano et al. (2021) used principal component analysis to synthesize a wide range of realistic faces from the BFM database and examined the effect of weight, age, gender, and height on the mask fit and peripheral gaps. In an extension of this work, Shoele and coworkers incorporated flow simulations within this framework (**Figure 4**), demonstrating leakage flows associated with different masks and a range of face shapes (Solano et al. 2022).

An interesting computational modeling–based study in this regard was conducted by Dbouk & Drikakis (2020), who modeled the FE of a surgical mask for a cough, including the Lagrangian dynamics of the respiratory aerosol particles (see **Figure 5**). The particle size range in their model was centered around a relatively large value of 70 μm (appropriate for a cough), and results indicate that despite a large gap around the entire periphery of the mask that ranged from 4 mm to 1.4 cm, the proportion of total droplets escaping from the mask was less than 20%. This result is consistent with the notion that large particles tend to reduce σ and move the FFE toward its upper bound (see Equation 1).

5.2. Modification of Expiratory Flows

In addition to modifying the aerosol loading of the expelled breath, the presence of the mask has a significant effect on the shape, direction, and persistence of the expiratory jet. The expiratory flow is often modelled as a jet flow, although the direction of the jet depends on the origin (mouth or nose), and the peak velocity and duration depend on the nature of the generating action (breathing,

$c_k = 2 \times 10^5$ $c_k = 10^4$ $c_k = 10^3$ $c_k = 10^2$

More porous
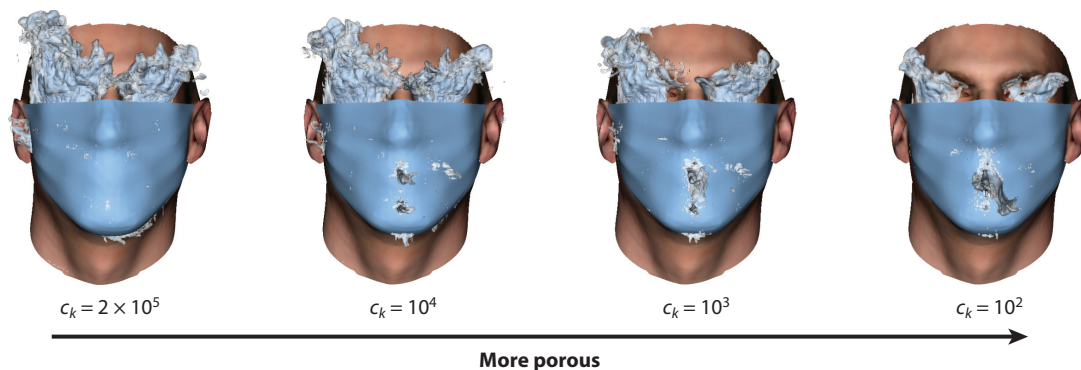
Figure 4

Effect of permeability c_k on the leakage flow predicted from a computational model that uses computational mechanics modeling of the mask to predict the mask conformation and peripheral leaks, as well as computational fluid dynamics to predict the resulting flow. Figure adapted from Solano et al. (2021) with permission of AIP Publishing.
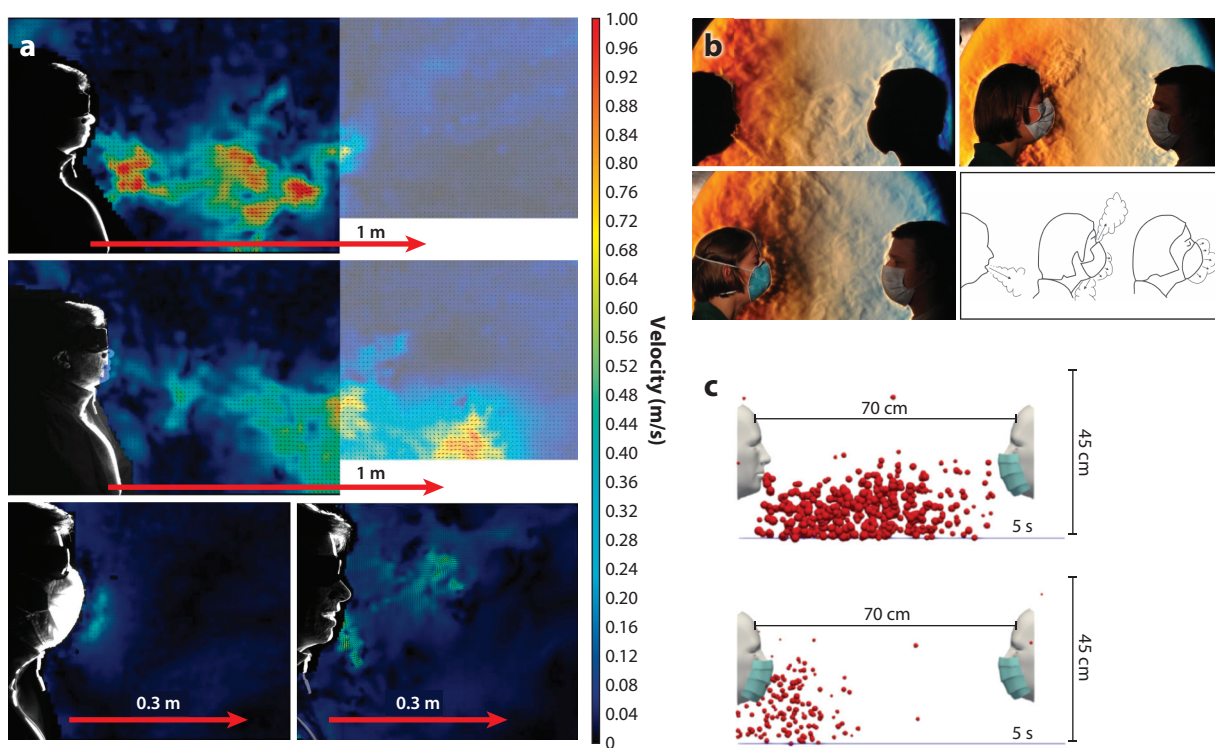
Figure 5

Visualizations of outward flows using different techniques. (*a*) Particle image velocimetry images of outward flows both with and without a mask. Panel *a* adapted from Kähler & Hain (2020) (CC BY 4.0). (*b*) Schlieren images of outward flow, highlighting the density differences between the warm breath and the cooler ambient air. Panel *b* images provided by G. Settles. (*c*) Visualization of simulated droplet densities during exhaled flows for situations with and without the host wearing a mask. Panel *c* adapted from Dbouk & Drikakis (2020) with permission of AIP Publishing.

speaking, singing, coughing, etc.). Although there have been earlier measurements of breathing patterns (Marr et al. 2008), the most extensive measurements are more recent, due to Abkarian et al. (2020), who used particle image velocimetry (PIV) to characterize the jet of steady outward breaths, as well as the differences in the jets that result from words being spoken. The components of speech associated with more steady breaths behaved much like a turbulent jet (the estimated Reynolds number based on the exit velocity and the diameter of the mouth varies between 700 and 7,000), with a propagation length L, which scaled roughly as $t^{1/2}$. In contrast, plosive events generated by phrases such as "Peter Piper..." generated individual vortex-like puffs that dominated at larger distances from the mouth, with a propagation length that scaled more like $L \sim t^{1/4}$. Singing, perhaps surprisingly, is not always accompanied by high expiratory velocities (Bourrianne et al. 2021a, Bahl et al. 2021) because a trained singer exerts extensive breath control, generating an acoustic signature that is not necessarily accompanied by a large volume of expelled air.

The overall flow pattern of the respiratory jet is modified substantially by mask wearing. Schlieren images by Tang et al. (2009) of heavy breathing and coughing events demonstrate qualitatively that the dominant flows with a mask are not necessarily through the mask, but through leakage paths at the top (beneath the eyes), bottom (under the chin), and sides (over the cheeks) (see **Figures 4** and **5**). The flow through these leakage routes depends on the specifics of the mask (Kähler & Hain 2020, Verma et al. 2020), the shape of the face, and the fit. Quantitative measurements of exhalation breaths by Bourrianne et al. (2021b) confirm the redirection of the primary flow upward when a surgical mask is worn during gentle breathing (commonly experienced by anyone who wears eyeglasses). However, strong breaths are still directed predominantly in the horizontal direction directly away from the face. For all kinds of breathing patterns, the air speed was reduced by approximately an order of magnitude, resulting in a reduced horizontal penetration distance. With reduced flow velocity, buoyancy effects become dominant earlier in the evolution of the expiratory jet and the expelled air rises, moving the aerosol cloud upward and away from other people in close proximity. This is an important secondary outward protection effect of face masks.

Recent computational modeling studies, in which the mask is represented by a porous layer, have also provided data and insights into both flow and droplet trajectories during coughing events (Khosronejad et al. 2020, Dbouk & Drikakis 2020). In all cases, the penetration of the expiratory jet was reduced by the masks, and velocities were observed to drop by an order of magnitude.

6. INTERACTION OF DROPLETS WITH FACE MASKS

There are several possible outcomes as droplet-laden air passes through the face mask material: The droplets can pass through unaffected, impact and rebound from the mask fibers, or impact and be fragmented into smaller droplets that can be absorbed fully or partially by the face mask material. All of these possible paths for interaction have implications for the protection afforded by face masks. While absorption of drops is an essential function of the mask, over time, it increases the resistance to through flow and may result in increased peripheral leakage. Fragmentation of droplets leads to decreased size and increased number density of the released aerosol particles, both of which are undesirable, as they lead to a longer-lasting droplet cloud.

The micrometer-scale flow physics of droplet impact on a variety of substrates is a long-studied area of multiphase flow that is beyond the scope of this review. As a particular application of this field, however, droplet impact on textiles has received recent attention, even prior to the COVID-19 pandemic. Zhang et al. (2018) explored this phenomenon using high-speed videography of a Newtonian liquid on an ordered (woven) substrate with both hydrophilic and hydrophobic surface chemistries, finding that the penetration or absorption of the droplet was largely characterized by a critical mesh size d_m that scaled with the impact Weber number, $d_m \sim d_p/We$, with

| $t = 0$ μs | $t = 100$ μs | $t = 250$ μs | $t = 450$ μs | $t = 750$ μs | $t = 950$ μs |

2,000 μm
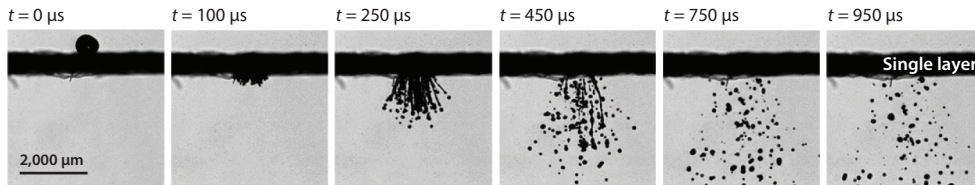
Single layer

Figure 6

High-speed photo sequence of a large droplet interacting with a mask, demonstrating the breakup of droplets as they pass through a single layer of mask material. Figure adapted from Sharma et al. (2021) (CC BY-NC 4.0).

$We = \rho U^2 d_\mathrm{p}/2\gamma$, where γ is the surface tension. This was largely corroborated by Sharma et al. (2021) for large $[\mathcal{O}(250)$ μm] droplets of a surrogate non-Newtonian fluid—representing a real-life coughing event—impacting a commercial surgical mask. With a sufficiently high impact velocity these droplets were observed to penetrate the mask layer and break up into smaller droplets via a Rayleigh–Plateau-type of interfacial instability (**Figure 6**). Multiple layers of mask material significantly reduced the probability of droplet penetration.

Karadimos & Ocone (2003) studied interaction between the droplet particles and fibers using computational models and observed changes in the FE over time due to the particle deposition on the fiber. The computational model of Dbouk & Drikakis (2020) is one of the few studies of this kind that have incorporated sticking, splashing/rebound, and penetration of droplets through the mask based on physics that is primarily determined by the nondimensional Weber and Laplace numbers.

7. EXPERIMENTAL APPROACHES: CHALLENGES AND OPPORTUNITIES

Although this field is changing rapidly, studies of the flow physics of masks and mask–droplet interactions have been dominated by experimental studies. The problem combines multiple complex phenomena that we have outlined in this review, including the behavior of polydisperse aerosol-laden air flows (with non-Newtonian liquid properties), pressure-driven flows through ordered and random fiber networks, the deformation and breakup of droplets in contact with porous mask materials, and the effects of surface charge on aerosol-laden gases. Quantitative characterization of each of these phenomena is challenging. Combining them into a coupled problem represents an even more daunting task.

As discussed earlier, characterization of mask materials—pressure drop and particle absorption as functions of flow rate—is a mature and well-trodden area of inquiry (Kwong et al. 2021). Nevertheless, questions in this domain remain unexplored, including more detailed understanding of the nonlinear pressure drop at higher flow rates (which is often modeled by the Forchheimer term), the change in material properties with use, and the effects of flow-induced deformations on different materials and on their hydrodynamic performance.

Measurements of the structure of the expiratory jet both with and without masks typically employ optical techniques. Schlieren imaging, which detects density changes (Settles 2001), was employed by Tang et al. (2009) to produce qualitative images of the flows associated with breathing and coughing, both with and without a face mask (**Figure 5**). Although the technique can yield quantitative information (e.g., Xu et al. 2017), it is better suited as a qualitative measure of the structure and extent of exhalation and requires specialized and carefully aligned optics (particularly for large-format fields of view, such as a human head). Furthermore, the Schlieren image also picks

up the natural thermal convection–induced flows set up by the (warm) body, and this complicates the analysis of the respiratory flow.

A distinct characteristic of the human breath is an elevated concentration of carbon dioxide (CO_2). Thus, imaging CO_2 concentration, using its strong absorption in the infrared (IR) part of the spectrum, can be used to quantify expiratory flows. Although an IR camera is required, this technique has the appeal that it does not require any other specialized equipment and is easy and safe to employ. Using CO_2 imaging, the reach and spreading of typical exhalation events have been quantified (Fei et al. 2005, Bourrianne et al. 2021b). CO_2 absorption imaging has two chief disadvantages: Firstly, although it accurately tracks the warm breath of exhalation, it does not directly measure droplets and, hence, the presence of potential pathogens. Secondly, the IR camera integrates the total concentration between the IR light source and the camera and, thus, can only give a planar description of the flow field.

The most quantitative and complex system to measure the flow associated with breathing and the effects of facial masks is PIV (Raffel et al. 2018). The field of interest is seeded with small droplets (either the naturally generated aerosols of the exhaled breath, or droplets generated by artificial means), and a pulsed laser sheet is used to illuminate a thin plane: for example, the symmetry plane of the head or a horizontal plane below the nostrils. The motion of the droplets is imaged using high-speed cameras, and correlation analysis techniques are used to compute the velocity field from the acquired image sequence. PIV has several appealing features for the measurement of exhalation events. Firstly, it gives detailed and quantitative velocity measurements. Secondly, it can be configured to measure a range of geometric configurations. Lastly, since droplets are the carriers of pathogenic viruses, PIV measurements (and associated particle analysis of the PIV images) directly measure the concentration, size distribution, velocity, and extent of the potentially infectious material.

While traditional PIV methods have attempted to generate small droplets that are passively carried by the flow, in the study of mask effectiveness, the paths of all droplets are relevant, whether they are passive tracers or inertial particles. Studies using an artificial aerosol cloud have quantified the nature of both the inhalation and exhalation breathing events (Abkarian et al. 2020), coughing (Zhu et al. 2006, VanSciver et al. 2011), and the leakage paths associated with masks (Bourrianne et al. 2021b), while naturally seeded flows tracking the motion of droplets expelled from the nose and mouth during coughing and sneezing events have been used used to characterize details of the direction and entrainment of the surrounding fluid, as well as the sedimentation of larger droplets (Bourouiba et al. 2014, Kähler & Hain 2020).

PIV does have limitations as well. The technique generally requires the use of high-power lasers, which are hazardous and difficult to set up. This makes the use of PIV systems in live-subject experiments challenging and, hence, limits the technique's usage in this particular application.

To date, there have not been many measurements of inhalation velocity fields. These flows are typically quite slow—due to the point-sink nature of the inhalation event—and, thus, difficult to distinguish from the weak convective currents always present in the ambient atmosphere. In addition, since the inward flow originates from the ambient room, the flow neither is naturally seeded nor contains elevated levels of CO_2; this necessitates artificial seeding of the atmosphere, which complicates the measurements, particularly when using human subjects.

8. COMPUTATIONAL MODELING: CHALLENGES AND OPPORTUNITIES

Computational models can provide insights into the key aspects of the flow physics of face masks, including filtration physics (Karadimos & Ocone 2003), perimeter leakage (Lei et al. 2010, 2012,

2013; Perić & Perić 2020; Solano et al. 2021), and expiratory flow modification (Dbouk & Drikakis 2020, Khosronejad et al. 2020, Leonard et al. 2020, Solano et al. 2022). Simulations that model the aerosol/droplet phase can even allow for the estimation of the inward/outward protection effectiveness (Dbouk & Drikakis 2020, Khosronejad et al. 2020, Kumar et al. 2020, Leonard et al. 2020, Xi et al. 2020). The key challenges to the accuracy and fidelity of the simulations are modeling the flow–mask interaction, perimeter leakage, and the droplet–mask interaction.

In most computational studies, the mask is treated as a porous material and the flow resistance through the mask is modeled by Darcy's law. Besides the uncertainty and variability of the permeability value of the mask material, the numerical implementation of Darcy's model over the relatively thin mask requires extra attention and validation.

For modeling perimeter leakage, the perimeter gap between the mask and face surface has to be known. Since the gap is typically very small [$\mathcal{O}(1 \text{ mm})$], measuring it in the laboratory setting is challenging. Alternatively, the gap may be quantified by using mechanics-based models of the mask fitting to the face (Lei et al. 2010, 2012, 2013). The gap size and profile are, however, strongly dependent on the face size and shape, as well as on the mask type (Solano et al. 2021). Finally, accurate prediction of the gap requires modeling the contact mechanics between the mask and the face, an ongoing challenge in all computational mechanics problems.

The droplet filtration model is an important component in quantifying the inward/outward protection effectiveness of the mask. Modeling droplet filtration in macroscale simulations is, however, nontrivial. Simple filtration models such as a single FE (Xi et al. 2020) or a model based on pore size (Kumar et al. 2020) have been used in previous studies. Dbouk & Drikakis (2020) considered additional mechanisms such as sticking and splashing/rebound and estimated the penetration of the droplets in a simplified manner based on the relevant nondimensional numbers. A multiscale simulation could be the way to introduce a more accurate filtration model.

9. SUMMARY

Even prior to 2020, researchers from a variety of scientific disciplines had analyzed the efficacy of face masks and established the physical principles that underpin the success of face masks as defense against respiratory infections. However, necessity is the mother of invention, and the COVID-19 pandemic has led to a torrent of research that has resulted in a notable improvement in our understanding of the various factors that determine the effectiveness of face masks. This progress has leveraged decades of fundamental research in fluid mechanics concerning droplet dynamics, aerosols, turbulent flows, and fluid–structure interactions; it has furthermore utilized many advanced state-of-the-art experimental and computational techniques. However, due to the complexity of the physical and physiological processes involved in the functioning of a face mask, a precise quantification of the effectiveness of face masks remains elusive, and this will undoubtedly continue to motivate future study. We hope that this brief review has put much of the classic and recent studies into a useful context. We further hope that this review will help guide future research, the development of more effective face masks, and decisions concerning public health and medical practice.

SUMMARY POINTS

1. COVID-19 has led to a massive surge in research on face mask flow physics and effectiveness, with studies employing the latest in experimental and computational methods.

2. These latest studies, combined with earlier research, have significantly improved our understanding of the physics that underpins face mask effectiveness.

3. Accurate estimates of the fitted filtration efficiency (FFE) of masks remain elusive given its complex dependencies on a variety of factors.

4. Peripheral leakage not only is the biggest challenge for the effectiveness of face masks but also is the factor that presents the highest complexity in the analysis of face mask performance.

DISCLOSURE STATEMENT

The authors are not aware of any biases that might be perceived as affecting the objectivity of this review.

ACKNOWLEDGMENTS

LITERATURE CITED

Abkarian M, Mendez S, Xue N, Yang F, Stone HA. 2020. Speech can produce jet-like transport relevant to asymptomatic spreading of virus. *PNAS* 117(41):25237–45

Asadi S, Wexler AS, Cappa CD, Barreda S, Bouvier NM, Ristenpart WD. 2019. Aerosol emission and superemission during human speech increase with voice loudness. *Sci. Rep.* 9(1):2348

Ather B, Mirza TM, Edemekong PF. 2020. Airborne precautions. In *StatPearls*. Treasure Island, FL: StatPearls. **https://www.ncbi.nlm.nih.gov/books/NBK531468/**

Bagheri G, Schlenczek O, Turco L, Thiede B, Stieger K, et al. 2021a. Exhaled particles from nanometre to millimetre and their origin in the human respiratory tract. medRxiv 2021.10.01.21264333. **https://doi.org/10.1101/2021.10.01.21264333**

Bagheri G, Thiede B, Hejazi B, Schlenczek O, Bodenschatz E. 2021b. An upper bound on one-to-one exposure to infectious human respiratory particles. *PNAS* 118(49):e2110117118

Bahl P, de Silva C, Bhattacharjee S, Stone H, Doolan C, et al. 2021. Droplets and aerosols generated by singing and the risk of coronavirus disease 2019 for choirs. *Clin. Infect. Dis.* 72(10):e639–41

Bałazy A, Toivola M, Adhikari A, Sivasubramani SK, Reponen T, Grinshpun SA. 2006. Do N95 respirators provide 95% protection level against airborne viruses, and how adequate are surgical masks? *Am. J. Infect. Control* 34(2):51–57

Bejan A. 2013. *Convection Heat Transfer*. Hoboken, NJ: Wiley

Bourouiba L. 2021. The fluid dynamics of disease transmission. *Annu. Rev. Fluid Mech.* 53:473–508

Bourouiba L, Dehandschoewercker E, Bush JWM. 2014. Violent expiratory events: on coughing and sneezing. *J. Fluid Mech.* 745:537–63

Bourrianne P, Kaneelil PR, Abkarian M, Stone HA. 2021a. Tracking the air exhaled by an opera singer. *Phys. Rev. Fluids* 6(11):110503

Bourrianne P, Xue N, Nunes J, Abkarian M, Stone HA. 2021b. Quantifying the effect of a mask on expiratory flows. *Phys. Rev. Fluids* 6(11):110511

Chao CYH, Wan MP, Morawska L, Johnson GR, Ristovski ZD, et al. 2009. Characterization of expiration air jets and droplet size distributions immediately at the mouth opening. *J. Aerosol Sci.* 40(2):122–33

Chen CC, Willeke K. 1992. Aerosol penetration through surgical masks. *Am. J. Infect. Control* 20(4):177–84

Corum J, Zimmer C. 2022. Tracking omicron and other coronavirus variants. *The New York Times*, accessed April 3. **https://www.nytimes.com/interactive/2021/health/coronavirus-variant-tracker.html**

Darquenne C. 2012. Aerosol deposition in health and disease. *J. Aerosol Med. Pulm. Drug Deliv.* 25(3):140–47

Das S, Sarkar S, Das A, Das S, Chakraborty P, Sarkar J. 2021. A comprehensive review of various categories of face masks resistant to COVID-19. *Clin. Epidemiol. Global Health* 12:100835

Dbouk T, Drikakis D. 2020. On respiratory droplets and face masks. *Phys. Fluids* 32(6):063303

Drewnick F, Pikmann J, Fachinger F, Moormann L, Sprang F, Borrmann S. 2021. Aerosol filtration efficiency of household materials for homemade face masks: influence of material properties, particle size, particle electrical charge, face velocity, and leaks. *Aerosol Sci. Technol.* 55(1):63–79

Dua K, Hansbro PM, Wadhwa R, Haghi M, Pont LG, Williams KA, eds. 2020. *Targeting Chronic Inflammatory Lung Diseases Using Advanced Drug Delivery Systems*. New York: Academic

Duguid J. 1946. The size and the duration of air-carriage of respiratory droplets and droplet-nuclei. *Epidemiol. Infect.* 44(6):471–79

Fei J, Zhu Z, Pavlidis I. 2005. Imaging breathing rate in the CO2 absorption band. In *Proceedings of the 27th Annual International Conference of the IEEE Engineering in Medicine and Biology Society*, pp. 700–5. New York: IEEE

Fennelly KP. 2020. Particle sizes of infectious aerosols: implications for infection control. *Lancet Respir. Med.* 8(9):914–24

Gralton J, Tovey E, McLaws ML, Rawlinson WD. 2011. The role of particle size in aerosolised pathogen transmission: a review. *J. Infect.* 62(1):1–13

Greenhalgh T, Jimenez JL, Prather KA, Tufekci Z, Fisman D, Schooley R. 2021. Ten scientific reasons in support of airborne transmission of SARS-CoV-2. *Lancet* 397(10285):1603–5

Grinshpun SA, Haruta H, Eninger RM, Reponen T, McKay RT, Lee SA. 2009. Performance of an N95 filtering facepiece particulate respirator and a surgical mask during human breathing: two pathways for particle penetration. *J. Occup. Environ. Hyg.* 6(10):593–603

Guarner J. 2020. Three emerging coronaviruses in two decades: the story of SARS, MERS, and now COVID-19. *Am. J. Clin. Pathol.* 153(4):420–21

Gupta JK, Lin CH, Chen Q. 2009. Flow dynamics and characterization of a cough. *Indoor Air* 19(6):517–25

Hill WC, Hull MS, MacCuspie RI. 2020. Testing of commercial masks and respirators and cotton mask insert materials using SARS-CoV-2 virion-sized particulates: comparison of ideal aerosol filtration efficiency versus fitted filtration efficiency. *Nano Lett.* 20(10):7642–47

Hinds WC. 1999. *Aerosol Technology: Properties, Behavior, and Measurement of Airborne Particles*. New York: Wiley. 2nd ed.

Johnson G, Morawska L, Ristovski Z, Hargreaves M, Mengersen K, et al. 2011. Modality of human expired aerosol size distributions. *J. Aerosol Sci.* 42(12):839–51

Ju JT, Boisvert LN, Zuo YY. 2021. Face masks against COVID-19: standards, efficacy, testing and decontamination methods. *Adv. Colloid Interface Sci.* 292:102435

Kähler CJ, Hain R. 2020. Fundamental protective mechanisms of face masks against droplet infections. *J. Aerosol Sci.* 148:105617

Karadimos A, Ocone R. 2003. The effect of the flow field recalculation on fibrous filter loading: a numerical simulation. *Powder Technol.* 137(3):109–19

Khosronejad A, Santoni C, Flora K, Zhang Z, Kang S, et al. 2020. Fluid dynamics simulations show that facial masks can suppress the spread of COVID-19 in indoor environments. *AIP Adv.* 10(12):125109

Koh XQ, Sng A, Chee JY, Sadovoy A, Luo P, Daniel D. 2022. Outward and inward protection efficiencies of different mask designs for different respiratory activities. *J. Aerosol Sci.* 160:105905

Kumar V, Nallamothu S, Shrivastava S, Jadeja H, Nakod P, et al. 2020. On the utility of cloth facemasks for controlling ejecta during respiratory events. arXiv:2005.03444 [physics.med-ph]

Kwong LH, Wilson R, Kumar S, Crider YS, Reyes Sanchez Y, et al. 2021. Review of the breathability and filtration efficiency of common household materials for face masks. *ACS Nano* 15(4):5904–24

Lai ACK, Poon CKM, Cheung ACT. 2012. Effectiveness of facemasks to reduce exposure hazards for airborne infections among general populations. *J. R. Soc. Interface* 9(70):938–48

Langmuir I. 1942. *Report on smokes and filters*. Tech. Rep. 865, Sect. I, Part IV, US Off. Sci. Res. Dev., Washington, DC

Lee H, Kim S, Joo H, Cho HJ, Park K. 2022. A study on performance and reusability of certified and uncertified face masks. *Aerosol Air Q. Res.* 22(2):210370

Lee KW, Liu BYH. 1982. Theoretical study of aerosol filtration by fibrous filters. *Aerosol Sci. Technol.* 1(2):147–61

Lee SA, Grinshpun SA, Reponen T. 2008. Respiratory performance offered by N95 respirators and surgical masks: human subject evaluation with NaCl aerosol representing bacterial and viral particle size range. *Ann. Occupat. Hyg.* 52(3):177–85

Lei Z, Yang JJ, Zhuang Z. 2010. Contact pressure study of N95 filtering face-piece respirators using finite element method. *Comput. Aided Des. Appl.* 7(6):847–61

Lei Z, Yang JJ, Zhuang Z. 2012. Headform and N95 filtering facepiece respirator interaction: contact pressure simulation and validation. *J. Occupat. Environ. Hyg.* 9(1):46–58

Lei Z, Yang JJ, Zhuang Z, Roberge R. 2013. Simulation and evaluation of respirator faceseal leaks using computational fluid dynamics and infrared imaging. *Ann. Occupat. Hyg.* 57(4):493–506

Leonard S, Atwood CW, Walsh BK, DeBellis RJ, Dungan GC, et al. 2020. Preliminary findings on control of dispersion of aerosols and droplets during high-velocity nasal insufflation therapy using a simple surgical mask. *Chest* 158(3):1046–49

Lepelletier D, Grandbastien B, Romano-Bertrand S, Aho S, Chidiac C, et al. 2020. What face mask for what use in the context of the COVID-19 pandemic? The French guidelines. *J. Hosp. Infect.* 105(3):414–18

Lewis D, et al. 2020. Mounting evidence suggests coronavirus is airborne—but health advice has not caught up. *Nature* 583(7817):510–13

Loudon RG, Roberts RM. 1967. Droplet expulsion from the respiratory tract. *Am. Rev. Respir. Dis.* 95(3):435–42

Mandavilli A. 2020. 239 experts with one big claim: The coronavirus is airborne. *New York Times*, July 4

Mao X, Hosoi AE. 2021. Estimating the filtration efficacy of cloth masks. *Phys. Rev. Fluids* 6(11):114201

Marr DR, Spitzer IM, Glauser MN. 2008. Anisotropy in the breathing zone of a thermal manikin. *Exp. Fluids* 44(4):661–73

Mittal R, Meneveau C, Wu W. 2020a. A mathematical framework for estimating risk of airborne transmission of COVID-19 with application to face mask use and social distancing. *Phys. Fluids* 32(10):101903

Mittal R, Ni R, Seo JH. 2020b. The flow physics of COVID-19. *J. Fluid Mech.* 894:F2

Morawska L, Milton DK. 2020. It is time to address airborne transmission of coronavirus disease 2019 (COVID-19). *Clin. Infect. Dis.* 71(9):2311–13

Mussap CJ. 2019. The plague doctor of Venice. *Int. Med. J.* 49(5):671–76

Oberg T, Brosseau LM. 2008. Surgical mask filter and fit performance. *Am. J. Infect. Control* 36(4):276–82

Pan J, Harb C, Leng W, Marr LC. 2021. Inward and outward effectiveness of cloth masks, a surgical mask, and a face shield. *Aerosol Sci. Technol.* 55(6):718–33

Papineni RS, Rosenthal FS. 1997. The size distribution of droplets in the exhaled breath of healthy human subjects. *J. Aerosol Med.* 10(2):105–16

Paysan P, Knothe R, Amberg B, Romdhani S, Vetter T. 2009. A 3D face model for pose and illumination invariant face recognition. In *2009 Sixth IEEE International Conference on Advanced Video and Signal Based Surveillance*, pp. 296–301. New York: IEEE

Perić R, Perić M. 2020. Analytical and numerical investigation of the airflow in face masks used for protection against COVID-19 virus—implications for mask design and usage. *J. Appl. Fluid Mech.* 13(6):1911–23

Pippin DJ, Verderame RA, Weber KK. 1987. Efficacy of face masks in preventing inhalation of airborne contaminants. *J. Oral Maxillofac. Surg.* 45(4):319–23

Pöhlker ML, Krüger OO, Förster JD, Berkemeier T, Elbert W, et al. 2021. Respiratory aerosols and droplets in the transmission of infectious diseases. arXiv:2103.01188 [physics.med-ph]

Raffel M, Willert CE, Scarano F, Kähler CJ, Wereley ST, Kompenhans J. 2018. *Particle Image Velocimetry*. Cham, Switz.: Springer Int.

Randall K, Ewing ET, Marr LC, Jimenez J, Bourouiba L. 2021. How did we get here: What are droplets and aerosols and how far do they go? A historical perspective on the transmission of respiratory infectious diseases. *Interface Focus* 11(6):20210049

Settles GS. 2001. *Schlieren and Shadowgraph Techniques*. Berlin: Springer

Sharma S, Pinto R, Saha A, Chaudhuri S, Basu S. 2021. On secondary atomization and blockage of surrogate cough droplets in single- and multilayer face masks. *Sci. Adv.* 7(10):eabf0452

Smith JD, MacDougall CC, Johnstone J, Copes RA, Schwartz B, Garber GE. 2016. Effectiveness of N95 respirators versus surgical masks in protecting health care workers from acute respiratory infection: a systematic review and meta-analysis. *CMAJ* 188(8):567–74

Solano T, Mittal R, Shoele K. 2021. One size fits all? A simulation framework for face-mask fit on population-based faces. *PLOS ONE* 16(6):e0252143

Solano T, Ni C, Mittal R, Shoele K. 2022. Perimeter leakage of face masks and its effect on the mask's efficacy. *Phys. Fluids* 34(5):051902

Steinle S, Sleeuwenhoek A, Mueller W, Horwell CJ, Apsley A, et al. 2018. The effectiveness of respiratory protection worn by communities to protect from volcanic ash inhalation. Part II: total inward leakage tests. *Int. J. Hyg. Environ. Health* 221(6):977–84

Tang JW, Liebner TJ, Craven BA, Settles GS. 2009. A schlieren optical study of the human cough with and without wearing masks for aerosol infection control. *J. R. Soc. Interface* 6(Suppl. 6):S727–36

Tang JW, Marr LC, Li Y, Dancer SJ. 2021. COVID-19 has redefined airborne transmission. *BMJ* 373:n913

Tuomi T. 1985. Face seal leakage of half masks and surgical masks. *Am. Ind. Hyg. Assoc. J.* 46(6):308–12

van der Sande M, Teunis P, Sabel R. 2008. Professional and home-made face masks reduce exposure to respiratory infections among the general population. *PLOS ONE* 3(7):e2618

Van Turnhout J, Hoeneveld W, Adamse JWC, Van Rossen LM. 1981. Electret filters for high-efficiency and high-flow air cleaning. *IEEE Trans. Ind. Appl.* (2):240–48

VanSciver M, Miller S, Hertzberg J. 2011. Particle image velocimetry of human cough. *Aerosol Sci. Technol.* 45(3):415–22

Verma S, Dhanak M, Frankenfield J. 2020. Visualizing the effectiveness of face masks in obstructing respiratory jets. *Phys. Fluids* 32(6):061708

Wang CC, Prather KA, Sznitman J, Jimenez JL, Lakdawala SS, et al. 2021. Airborne transmission of respiratory viruses. *Science* 373(6558):eabd9149

Wells WF. 1934. On air-borne infection: study II. Droplets and droplet nuclei. *Am. J. Epidemiol.* 20(3):611–18

Xi J, Si XA, Nagarajan R. 2020. Effects of mask-wearing on the inhalability and deposition of airborne SARS-CoV-2 aerosols in human upper airway. *Phys. Fluids* 32(12):123312

Xie X, Li Y, Chwang A, Ho P, Seto W. 2007. How far droplets can move in indoor environments—revisiting the Wells evaporation–falling curve. *Indoor Air* 17(3):211–25

Xu C, Nielsen PV, Liu L, Jensen RL, Gong G. 2017. Human exhalation characterization with the aid of schlieren imaging technique. *Build. Environ.* 112:190–99

Zangmeister CD, Radney JG, Vicenzi EP, Weaver JL. 2020. Filtration efficiencies of nanoscale aerosol by cloth mask materials used to slow the spread of SARS-CoV-2. *ACS Nano* 14(7):9188–200

Zhang G, Quetzeri-Santiago MA, Stone CA, Botto L, Castrejón-Pita JR. 2018. Droplet impact dynamics on textiles. *Soft Matter* 14(40):8182–90

Zhu S, Kato S, Yang JH. 2006. Study on transport characteristics of saliva droplets produced by coughing in a calm indoor environment. *Build. Environ.* 41(12):1691–702

Contents

Indexes

Errata

An online log of corrections to *Annual Review of Fluid Mechanics* articles may be found at http://www.annualreviews.org/errata/fluid